Mechanisms of Action of the Bactericidal/Permeability-Increasing Protein BPI on Endotoxin and Phospholipid Monolayers and Aggregates†

Andre Wiese,‡ Klaus Brandenburg,‡ Buko Lindner,‡ Andra B. Schromm,‡ Stephen F. Carroll,§ Ernst Th. Rietschel,‡ and Ulrich Seydel*,‡

Department of Immunochemistry and Biochemical Microbiology, Center for Medicine and Biosciences, Research Center Borstel, Parkallee 10, D-23845 Borstel, Germany, and XOMA Corporation, 2910 Seventh Street, Berkeley, California 94710

Received January 24, 1997; Revised Manuscript Received April 24, 1997⊗

ABSTRACT: We have investigated the mechanisms of interaction of the recombinant N-terminal portion of bactericidal/permeability-increasing protein, $rBPI_{21}$, with lipopolysaccharide (LPS) isolated from enterobacterial deep rough mutant strains. Experimentally, the ability of $rBPI_{21}$ to form monolayers at the air/water interface and its action on lipid monolayers were analyzed. We have further studied the interaction of $rBPI_{21}$ with aggregates from phospholipids and Re mutant LPS by infrared and resonance energy transfer spectroscopy and laser Doppler velocimetry. From monolayer experiments, the molecular area of a single $rBPI_{21}$ molecule was estimated to be about 12 nm^2. At lateral pressures of $\leq$25 mN/m, $rBPI_{21}$ incorporated into monolayers from negatively charged LPS and phosphatidylglycerol (PG) but not into those from neutral phosphatidylcholine. $rBPI_{21}$ incorporated not only into monolayers but also into liposomes made from or containing negatively charged phospholipids, reducing the absolute value of the ζ-potential of LPS and PG aggregates. Furthermore, due to intercalation, $rBPI_{21}$ caused the rigidification of the acyl chains of lipids in the gel as well as in the fluid phase and significantly immobilized their phosphate groups. High concentrations of Mg^{2+} ions were found to have a protective effect against the action of $rBPI_{21}$. On the basis of these results, the biophysical characteristics of $rBPI_{21}$ are discussed and a model is proposed as to how the $rBPI_{21}$-induced influence on lipid monolayers and bilayers could explain $rBPI_{21}$-mediated effects on the bacterial membrane.

The bactericidal/permeability-increasing protein (BPI)[1] belongs to the group of antibacterial peptides of polymorphonuclear neutrophils (PMN) capable of killing bacteria by oxygen-independent mechanisms. It is located in the azurophilic granules of neutrophils (Weiss & Olsson, 1987) and constitutes an approximately 55 kDa cationic protein with a selectivity toward Gram-negative bacteria (Weiss et al., 1978; Elsbach et al., 1979), most likely due to its strong affinity for lipopolysaccharides (LPS) (Gazzano-Santoro et al., 1992, 1995), the major components of the outer leaflet of the outer membrane of Gram-negative bacteria. LPS, which consist of an oligo- or polysaccharide moiety and a covalently linked lipid component, termed lipid A, anchoring the LPS in the outer membrane (Rietschel et al., 1994), is a dominant initiator of the pathophysiological, i.e., endotoxic, effects of invasive Gram-negative bacteria and a target for antibacterial drugs interacting with the microbial cell surface. A close correlation has been found between endotoxin as the inciting agent and the production of inflammatory mediators, the accumulation of which is causally related with the symptoms of Gram-negative bacterimea and septic shock (Brandtzaeg, 1996). For BPI, beside its bactericidal effects an endotoxin-neutralizing activity was described (Weiss et al., 1992; Elsbach & Weiss, 1993). Due to this double function, killing of invading bacteria and detoxifying LPS, BPI represents a candidate for antiseptic therapeutics.

Interestingly, most of the antibacterial and LPS-binding activity of holo-BPI is found in 20−25 kDa N-terminal fragments of the protein (Ooi et al., 1987, 1991; Capodici et al., 1994; Gazzano-Santoro et al., 1992; Horwitz et al., 1996). Furthermore, $rBPI_{21}$, representing a recombinant 21 kDa protein and corresponding to amino acids 1−193 of N-terminal human BPI (with the exception that a cysteine is replaced by an alanine at position 132), is bactericidal and binds to and thereby neutralizes endotoxin (Horwitz et al., 1996). N-terminal fragments of BPI also inhibit LPS-induced E-selectin expression and reduce NF-κB activation in LPS-stimulated endothelial cells (Huang et al., 1995).

Although various studies with BPI and its fragments have been performed concerning antimicrobial activity (Weiss et al., 1975, 1978, 1984; Elsbach & Weiss, 1993; Capodici et al., 1994), LPS binding (Gazzano-Santoro et al., 1992, 1995; Capodici et al., 1994), LPS neutralization (Ooi et al., 1991;

† This work was financially supported by the German Federal Minister of Education, Science, Research and Technology (BMBF Grant 01 KI 9471), the Deutsche Forschungsgemeinschaft (SFB 367, Projects B2 and B8, and SFB 470, Projects B4 and B5), and the Fonds der Chemischen Industrie (to E.Th.R.).

* To whom correspondence should be addressed.

‡ Research Center Borstel.

§ XOMA Corporation.

⊗ Abstract published in *Advance ACS Abstracts,* August 1, 1997.

[1] Abbreviations: LPS, lipopolysaccharide; F515 LPS, lipopolysaccharide of the *Escherichia coli* Re mutant strain F515; R45 LPS, lipopolysaccharide of the *Proteus mirabilis* Re mutant strain R45; BPI, bactericidal/permeability-increasing protein; $rBPI_{23}$, 23 kDa N-terminal fragment of bactericidal/permeability-increasing protein; $rBPI_{21}$, 21 kDa N-terminal fragment of bactericidal/permeability-increasing protein; PMN, polymorphonuclear neutrophils; PMB, polymyxin B; PMBN, polymyxin B nonapeptide; PG, phosphatidylglycerol; PC, phosphatidylcholine; PE, phosphatidylethanolamine; DMPG, dimyristoylphosphatidylglycerol; DMPC, dimyristoylphosphatidylcholine; NBD-PE, *N*-(7-nitro-2,1,3-benzoxadiazol-4-yl)phospatidylethanolamine; Rh-PE, *N*-(rhodamine B sulfonyl)phosphatidylethanolamine; RET, resonance energy transfer; PBS, phosphate-buffered saline; T_c, phase transition temperature

S0006-2960(97)00176-1 CCC: $14.00

Elsbach & Weiss, 1993), experiments in animals (Kartalija et al., 1995; Koyama et al., 1995; Lechner et al., 1995; Hansbrough et al., 1996), and human trials (de Winter et al., 1995), the biophysical parameters as the ability of BPI to form monolayers at the air/water interface, its molecular area, and the mechanisms of its interaction with lipids remain to be defined.

Here, we have studied the behavior of suspensions of $rBPI_{21}$, the BPI fragment of highest therapeutic interest (Ammons & Mallari, 1996; Meijer et al., 1997; Kirsch et al., 1997), and the interaction of $rBPI_{21}$ with lipid monolayers and aggregates (the term aggregate is also synonymously used for liposome). To acquire information on the lipid specificity of $rBPI_{21}$, we have performed pressure/area measurements on monolayers made from LPS and charged and uncharged phospholipids. Determination of the ζ-potential of LPS and PG aggregates in the absence and presence of $rBPI_{21}$ gave information on its influence on the surface potential and, therefore, on its binding. These determinations were supplemented by resonance energy transfer experiments to study the intercalation of $rBPI_{21}$ into aggregates made from various phospholipids and from LPS. The interaction of $rBPI_{21}$ with LPS and with various phospholipids was described by determining the acyl chain and phosphate mobilities with Fourier-transform infrared spectroscopy. For the interpretation of the data obtained on the action of $rBPI_{21}$, earlier results on the interaction of the decapeptide polymyxin B (PMB) and its nonapeptide (PMBN) with membrane systems (Schröder et al., 1992) were used by way of comparison.

The results of the present study allowed us to determine the following properties of $rBPI_{21}$. First, $rBPI_{21}$ forms a monolayer at the air/water interface with a maximal lateral pressure of about 35 mN/m, the molecular area of the molecule being about 12 nm^2 at a surface pressure of 25 mN/m. Second, $rBPI_{21}$ binds to negatively charged lipid surfaces, followed by its insertion into the lipid matrix causing rigidification of the acyl chains of the lipids. Third, the binding and insertion of $rBPI_{21}$ leads to significant changes of the surface potential of the lipids.

These changes in membrane characteristics are assumed to play an important role for the permeability-increasing and bactericidal activity of BPI.

MATERIALS AND METHODS

Materials

Lipids and Other Chemicals. LPS of the deep rough (Re) mutant of *Escherichia coli* strain F515 (for chemical structure, see Figure 1) and from the deep rough mutant of *Proteus mirabilis* strain R45 were used in the experiments with LPS monolayers and aggregates. LPS were extracted by the phenol/chloroform/petroleum ether method (Galanos et al., 1969), purified, lyophilized, and dialized. Dialysis guaranteed that the LPS samples contained less than 1 divalent cation per 100 LPS molecules as proven by atomic absorption spectroscopy. Egg phosphatidylcholine (PC), phosphatidylglycerol (PG) from egg yolk, and phosphatidylethanolamine (PE) from *E. coli* were obtained from Sigma Chemical Co. (St. Louis, MO). Dimyristoylphosphatidylglycerol (DMPG) and dimyristoylphosphatidylcholine (DMPC) were purchased from Avanti Polar Lipids (Alabaster, AL)

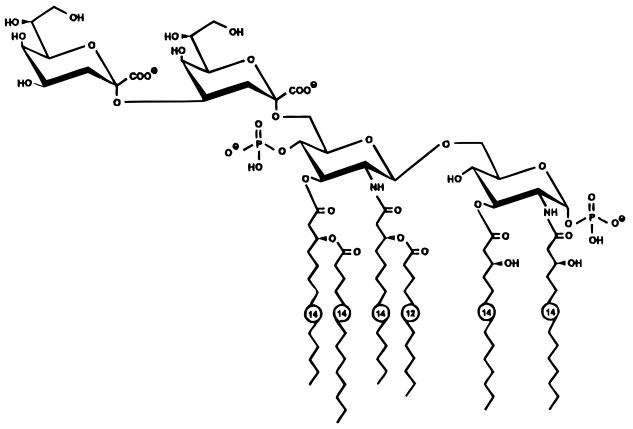

FIGURE 1: Chemical structure of LPS of the deep rough *Escherichia coli* Re mutant strain F515 [according to Zähringer et al. (1985)].

and used without further purification. The fluorescent dyes *N*-(7-nitro-2,1,3-benzoxadiazol-4-yl)-PE (NBD-PE) and *N*-(rhodamine B sulfonyl)-PE (Rh-PE) were purchased from Molecular Probes (Eugene, OR).

Proteins. $rBPI_{21}$, a recombinant N-terminal fragment of human BPI, was produced and purified as described (Horwitz et al., 1996) and was obtained as a sterile, nonpyrogenic solution at a concentration of 3 mg/mL in citrate-buffered saline (150 mM NaCl and 5 mM sodium citrate, pH 5) without detergents or stabilizers. The $rBPI_{21}$ samples were aliquoted, frozen in liquid nitrogen, and stored at −70 °C. Before use, the samples were thawed, kept at 4 °C, and used within 1 week. The bactericidal activity of $rBPI_{21}$ was tested prior to use against *E. coli* strain J5 as described by Capodici et al. (1994). Polymyxin B and its nonapeptide were obtained from Boehringer (Mannheim, Germany).

Methods

Film Balance Measurements. The molecular area of an $rBPI_{21}$ molecule was estimated from pressure/area isotherms of $rBPI_{21}$ solutions at various concentrations (5.0−17.9 nM) in an aqueous subphase of 150 mM NaCl and 5 mM HEPES at pH 7, which were recorded with a thermostated Langmuir film balance equipped with a Wilhelmy system at 37 °C. $rBPI_{21}$ was added to the subphase, and after 2 h, pressure/area isotherms were recorded at a compression rate of 1.5 mm^2/s. The molecular area of the $rBPI_{21}$ molecules at a given lateral pressure was estimated from the slope of a plot of the number of $rBPI_{21}$-molecules added to the subphase as a function of the respective film area (Schwarz & Taylor, 1995). The incorporation of the protein into lipid monolayers from the aqueous subphase was studied with monolayers spread from 1 mM chloroform solutions of DMPG and DMPC, respectively, and with chloroform/methanol (9:1 v/v) solutions of LPS. The experiments were run at 37 °C. Prior to isotherm recording, monolayers were equilibrated at zero pressure for 5 min to allow evaporation of the solvent. The monolayers were compressed to a lateral pressure of 25 mN/m [this value was chosen because it is within the range of lateral pressures present in biological bilayer membranes (Marcelja, 1974; Blume, 1979)]. $rBPI_{21}$ was added to the subphase and the compression was continued after 30 min to a final value of 40 mN/m. The subsequent expansion isotherms were recorded at an expansion rate of 3.0 mm^2/s. To examine the influence of Mg^{2+} ions, expansion isotherms were recorded in the absence or presence of $MgCl_2$ (0 or 40

mM) in the subphase. F515 LPS monolayers were first spread on the respective subphase and compressed to a lateral pressure of 40 mN/m (compression rate 3.0 mm^2/s), and then 12 nM $rBPI_{21}$ was added to the subphase. Thirty minutes after $rBPI_{21}$ addition, expansion isotherms were recorded at an expansion rate of 0.6 mm^2/s to allow incorporation of $rBPI_{21}$ during the expansion process. As a control, expansion isotherms were recorded after an equilibration period of 30 min at 40 mN/m without adding $rBPI_{21}$. Because of the long period of time (approximately 4 h) needed, these experiments were done at a temperature of 20 °C to reduce evaporation of the subphase and to avoid protein degradation.

ζ-Potential Measurements. Fixed charges within the headgroups of the lipid molecules provoke an electrical potential at each surface of the lipid bilayer with respect to the surrounding bathing solution, the surface potential [for review on membrane electrostatics see also Cevc (1990)]. At neutral pH, of the phospholipids only the phosphatidylglycerol molecule carries one negative charge, whereas each F515 LPS molecule carries four negative charges. The resulting surface charge densities are -0.52 As/m^2 (-3.25 e_0/nm^2) for F515 LPS and -0.05 As/m^2 (-0.31 e_0/nm^2) for the phospholipid mixture resembling the inner leaflet of the outer membrane, respectively, since the molecular cross-section of an F515 LPS molecule is 1.23 nm^2 and that of a diacyl phospholipid is 0.55 nm^2 (determined from monolayer isotherms with a film balance). In the R45 LPS molecule, the 4′-phosphate and the first Kdo are non-stoichiometrically substituted with 4-amino-4-deoxy-L-arabinopyranose (Vinogradov et al., 1994). As could be shown by MALDI mass spectroscopy (data not shown), total substitution is approximately 50%, resulting in about 3 negative charges/molecule and a surface charge density of -0.38 As/m^2, corresponding to -2.36 e_0/nm^2 (molecular area of 1.27 nm^2).

To study the influence of $rBPI_{21}$ on surface potential, we determined the ζ-potential (which is related to the surface potential of lipid aggregates) by measuring their electrophoretic mobilities [for review see Cevc (1993)]. The ζ-potential was calculated according to the Helmholtz−Smoluchowski equation (Hunter, 1981) from the electrokinetic mobility of lipid aggregates, measured by laser Doppler anemometry. The measurements were performed on a ZetaSizer 4 (Malvern Instruments GmbH, Herrsching, Germany) at 20 °C and a driving electric field of 19.2 V/cm. Lipid aggregates were prepared from 0.5 mM aqueous dispersions of F515 LPS or PG in buffer solution (2.5 mM Tris/HCl and 1 mM CsCl, pH 7) by sonification for 20 min in an ultrasonic bath at 40 °C. Subsequently, the preparation was allowed to equilibrate overnight at 4 °C before experiments were started. $rBPI_{21}$ and PMBN were solved in aqueous solutions of 150 mM NaCl and 5 mM sodium citrate at concentrations of 95.2 μM and 1 mM, respectively. Samples (2 mL) were prepared by diluting the lipid stock solution with buffer to a final concentration of 75 μM, and the ζ-potential was monitored in dependence on increasing amounts of $rBPI_{21}$ and PMBN. Investigations into the influence of $rBPI_{21}$ on the ζ-potential of R45 LPS aggregates were not possible, because the protein led to immediate precipitation of the aggregates.

Resonance Energy Transfer Spectroscopy. The resonance energy transfer (RET) technique is used here as a probe dilution assay (Struck et al., 1981) to obtain information on the incorporation of $rBPI_{21}$ into aggregates (liposomes) made from various phospholipids and F515 LPS. Respective experiments with R45 LPS could not be performed for reasons as above. For the RET measurements, PC, PG, or F515 LPS aggregates were double-labeled with NBD-PE and Rh-PE. The fluorescent dyes were dissolved together with PC, PG, or F515 LPS in chloroform in molar ratios [lipid]:[NBD-PE]:[Rh-PE] of 100:1:1. The solvent was evaporated under a stream of nitrogen, and the lipids were resuspended in phosphate-buffered saline (PBS) at pH 7.2, mixed thoroughly, and sonicated with a Branson sonicator for 1 min (1 mL solution). Subsequently, the preparation was cooled for 30 min at 4 °C, heated for 30 min at 56 °C, and recooled to 4 °C. Preparations were stored at 4 °C overnight prior to measurement. A preparation of 900 μL of the double-labeled PC, PG, or F515 LPS aggregates (0.1 mM) at 37 °C was excited at 470 nm (excitation wavelength of NBD-PE) and the intensities of the emission light of NBD-PE (531 nm) and Rh-PE (593 nm) were measured simultaneously on the fluorescence spectrometer SPEX F1T11 (SPEX Instruments, Edison, NY) in two separate emission channels. The protein was added after 50 s to a final concentration of 50 μg/mL. Intercalation then led to changes in fluorescence intensities as a function of time (increase of donor signal, decrease of acceptor signal; for the sake of clarity, in the Results section only the donor signal is plotted). To obtain identical intensities before the addition of $rBPI_{21}$, the emission intensities in both channels were recorded for 50 s under continuous stirring to determine the base line, and the slits of the two channels were adjusted to yield identical intensities (180 000 cps). To exclude different fluorescence behavior of the dyes in the phospholipid and LPS aggregates, i.e., that the incorporation of identical amounts of unlabeled molecules would lead to different changes in the fluorescence intensities, the two aggregate systems were calibrated. For this, known amounts of unlabeled molecules were incorporated in the labeled aggregates. This step required chloroform solubility of the molecules used for calibration and thus excluded $rBPI_{21}$. Instead we used the phospholipids PC and PE. The admixture of identical amounts of each of these phospholipids to the labeled phospholipid and LPS aggregates, respectively, led to changes in fluorescence intensity, which were comparable for PC and PE but different for the two aggregate systems. Therefore, to render the results on $rBPI_{21}$ incorporation into the two aggregate systems comparable, the quotient of the fluorescence intensities after the addition of $rBPI_{21}$ and the intensities achieved with aggregates containing—beside the double-labeled lipids—50% of unlabeled PC or PE was taken as a measure.

FTIR Spectroscopy. FTIR spectroscopic measurements were applied to detect changes of characteristics of vibrational bands—i.e., their position—of functional groups of the composing lipids upon interaction with externally applied compounds (here, $rBPI_{21}$ and PMB), which renders information on the interaction between the latter and the lipid matrix. All lipid samples were prepared as aqueous suspensions in 5 mM HEPES buffer, pH 7, at high water content (20 mM lipid corresponding to approximately 96% water content). For this, the lipids were suspended directly in distilled water and were temperature-cycled twice between 4 and 70 °C and then stored at 4 °C for at least 12 h before measurement. After the preparation of the LPS or phospholipid aggregates, PMB or $rBPI_{21}$ was added in appropriate concentrations and

the mixtures were briefly vortexed at 37 °C. Measurements were performed on a Bruker FTIR spectrometer IFS55 (Bruker, Karlsruhe, Germany). The lipid samples were placed in a CaF_2 cuvette separated by a 12.5 μm thick Teflon spacer. Temperature scans were performed automatically in the range from 10 to 65−80 °C with a heating rate of 3 °C/5 min. Every 3 °C, 50 interferograms were accumulated, apodized, Fourier-transformed, and converted to absorbance spectra.

The $\beta \leftrightarrow \alpha$ gel to liquid crystalline phase transition of the hydrocarbon chains was determined by monitoring the symmetric stretching vibration of the methylene groups $\nu_s(CH_2)$. The peak position of $\nu_s(CH_2)$ is known to lie at approximately 2850 cm^{-1} in the gel phase and to shift at a lipid-specific temperature (phase transition temperature) T_c to 2852.0−2852.5 cm^{-1} in the liquid crystalline phase (Mantsch & McElhaney, 1991). The interaction of the protein with the lipid headgroups was studied by monitoring the antisymmetric stretching vibration of the negatively charged phosphate groups $\nu_{as}(PO_2^-)$ in the range from 1220 to 1260 cm^{-1}.

The evaluation of the band parameters (peak position and intensity) was performed after subtraction of superimposed water bands. Thus, the position of the peak maxima could be determined with a precision of better than 0.1 cm^{-1}.

Because in all experimental systems relatively large amounts of protein have to be introduced and the supply of recombinant protein was not unlimited, each experiment was repeated at least twice. Deviations of more than 5% have never been observed.

RESULTS

Surface Activity. When amphiphilic or hydrophobic molecules are added to an aqueous subphase, they tend to adsorb to the air/water interface and thus reduce the surface tension of the subphase. On a film balance, the generated films (monolayers) can be compressed, and the lateral pressure at any surface area can be related to the surface tension for a given subphase temperature (the lateral pressure corresponds to the difference between the surface tensions of a subphase in the absence and presence of a monolayer). From the pressure/area curves at a given temperature (isotherms), the surface area occupied by the surfactant molecules (area per molecule) at a given lateral pressure can be calculated. Furthermore, the incorporation of molecules from the subphase into a monolayer can be studied.

Aqueous suspensions of $rBPI_{21}$ led to the formation of $rBPI_{21}$ monolayers at the air/water interface. In Figure 2A pressure/area isotherms of $rBPI_{21}$ monolayers on $rBPI_{21}$ suspensions of different concentrations in 5 mM HEPES subphases containing 150 mM NaCl are presented. At low $rBPI_{21}$ concentrations, an exponential increase of lateral pressure with decreasing film area was observed, whereas at higher $rBPI_{21}$ concentrations, the lateral pressure showed an initial linear increase that slowed at higher lateral pressures above 30 mN/m. In Figure 2B the relation between the number of molecules added to the subphase and the occupied area at a lateral pressure of 25 mN/m is plotted. A regression analysis showed that the molecular area of one $rBPI_{21}$ molecule at the air/water interface was 11.8 ± 3.9 nm^2.

For LPS and DMPG monolayers compressed to 25 mN/m, the addition of $rBPI_{21}$ into the subphase led to an increase

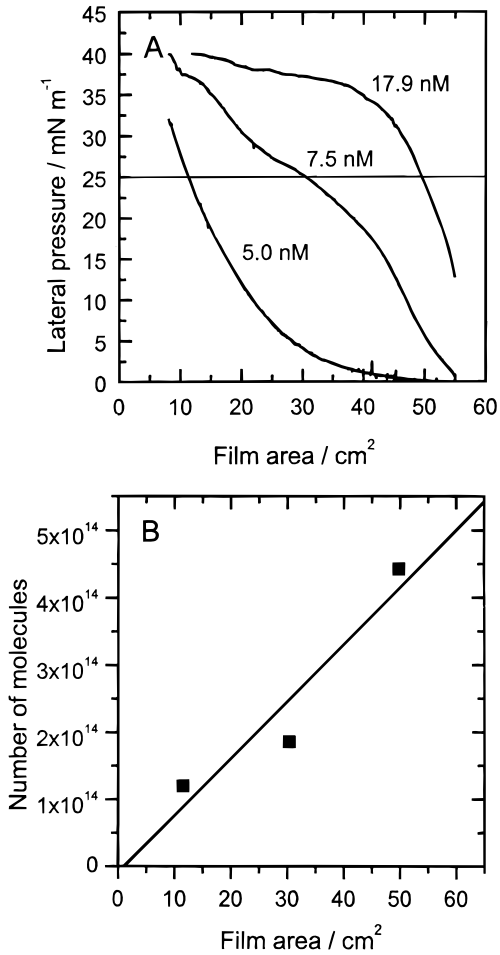

FIGURE 2: (A) Pressure/area isotherms of $rBPI_{21}$ monolayers on $rBPI_{21}$ suspensions of different concentrations. Subphase: 150 mM NaCl, 5 mM HEPES-buffered at pH 7, $T = 37$ °C. (B) Estimation of the molecular area of $rBPI_{21}$ molecules. Number of molecules added to the subphase is plotted as a function of the occupied area at a lateral pressure of 25 mN/m (squares). From a regression analysis (line), the molecular area was calculated to be 11.8 ± 3.9 nm^2.

in film area (Figure 3), whereas for a DMPC monolayer under otherwise identical conditions no significant change in film area could be observed (Figure 3B). The increase in film area was most pronounced for the F515 LPS monolayers, indicating the strongest incorporation. The incorporation into R45 LPS monolayers was half that into F515 LPS but comparable to that into DMPG monolayers. For an understanding of these observations it should be considered that phospholipid monlayers contain twice the number of molecules per unit area as do LPS monolayers.

To investigate the influence of Mg^{2+} on the interaction of $rBPI_{21}$ with LPS monolayers, expansion isotherms of F515 LPS monolayers were recorded in the absence and presence of 40 mM $MgCl_2$ and in the absence and presence of 12 nM $rBPI_{21}$ (Figure 4). Clearly, the addition of $rBPI_{21}$ to the subphase led to a much more pronounced increase in film area in the absence than in the presence of $MgCl_2$. It should be noted, however, that $MgCl_2$ itself caused a slight increase in film area.

ζ-Potential. The interaction of externally applied substances with the lipid bilayer may induce changes in the surface potential, in particular when these substances carry electric charges. The determination of changes of the surface potential following the interaction with polycationic mol-

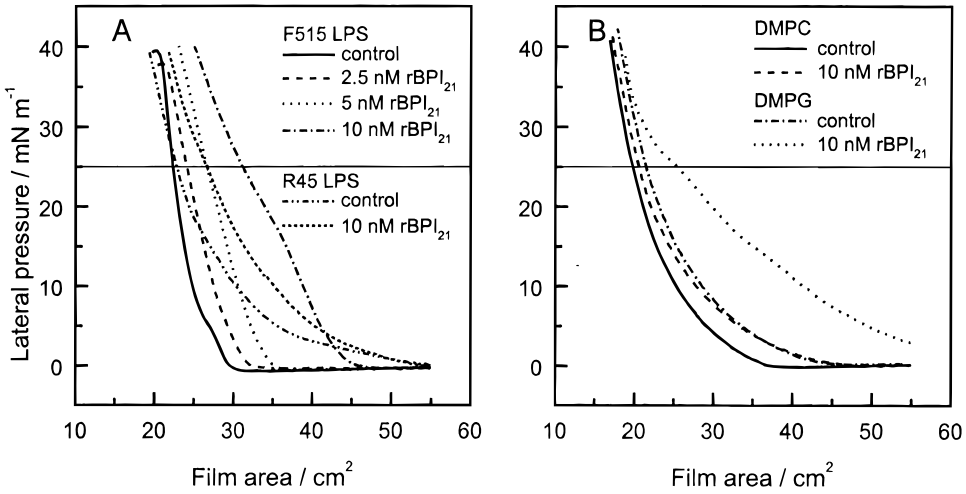

FIGURE 3: Expansion isotherms of LPS monolayers (A) and phospholipid monolayers (B) before and after the addition of different amounts of $rBPI_{21}$ to the subphase at a lateral pressure of 25 mN/m (expansion rate 3.0 mm/s). Subphase: 150 mM NaCl, 5 mM HEPES-buffered at pH 7, $T = 37$ °C.

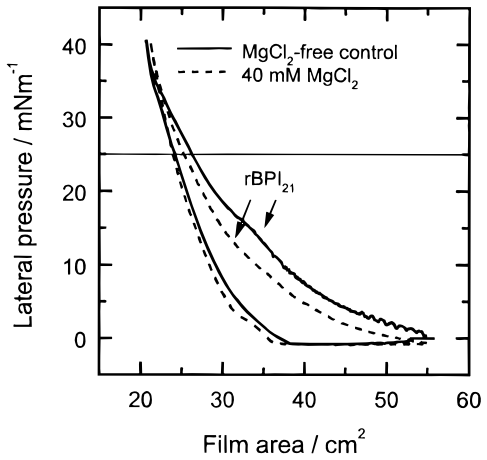

FIGURE 4: Expansion isotherms (expansion rate 0.6 mm/s) of F515 LPS monolayers in the absence and presence of 40 mM $MgCl_2$ and before and after the addition of 12 nM $rBPI_{21}$ to the subphase at a lateral pressure of 40 mN/m. The arrows mark the isotherms after $rBPI_{21}$ addition. Subphase: 150 mM NaCl, 5 mM HEPES-buffered at pH 7, $T = 20$ °C.

ecules thus provides direct information regarding the binding process. To assess this parameter the ζ-potential was determined in the absence and presence of $rBPI_{21}$ and Mg^{2+}. Comparative measurements were performed with PMBN, which is known to attach to the hydrophilic and negatively charged lipid headgroups and not to intercalate deeply into the hydrophobic moiety (Beurer et al., 1988). PMBN instead of PMB has been chosen to get results on the surface potential, which can be used for determination of the potential profile in bilayer membranes (Wiese et al., 1997). In those experiments PMB could not be applied because of its permeabilizing activity (Schröder et al., 1992).

The influence of $rBPI_{21}$ and PMBN on the ζ-potential of F515 LPS and PG aggregates is shown in Figure 5. The addition of increasing amounts of $rBPI_{21}$ to a suspension of F515 LPS aggregates (Figure 5A) led to a nearly linear increase of the ζ-potential from approximately −57 mV and a reversal of the ζ-potential up to a saturation value of +12 mV, which was reached at a molar ratio of [$rBPI_{21}$]:[F515 LPS] ≈ 1:10. In contrast, much higher amounts of PMBN were needed to reach a saturation value (≈0 mV) that is significantly lower than that observed with $rBPI_{21}$.

The interaction of $rBPI_{21}$ and PMBN with PG aggregates led to effects similar to those seen with F515 LPS (Figure 5B), but at much lower peptide concentrations. The saturation values (≈+13 mV for $rBPI_{21}$ and ≈+3 mV for PMBN) were reached at molar ratios of [$rBPI_{21}$]:[PG] ≈ 1:20 and [PMBN]:[PG] ≈ 1:4.

Resonance Energy Transfer. To examine the intercalation of $rBPI_{21}$ into lipid- or LPS membrane systems, we also determined the energy transfer between two fluorescent markers. After the addition of 2.4 μM $rBPI_{21}$ to a 0.1 mM suspension of double-labeled F515 LPS or PG aggregates, an increase in fluorescence intensity of the donor signal (indicative for $rBPI_{21}$ incorporation) was observed (Figure 6). For PC aggregates under otherwise identical conditions, no incorporation of $rBPI_{21}$ was observed as indicated by a slight decrease in intensity, which was due to dilution effects. For a comparison of the amount of $rBPI_{21}$ incorporated into the different lipid aggregates, the signals after $rBPI_{21}$ addition were normalized to those for a common preparation with a known amount of unlabeled PC or PE (see Materials and Methods). Here (Figure 6B), only the results for calibration with PC are depicted, showing that more $rBPI_{21}$ was incorporated into F515 LPS than into PG aggregates.

FTIR Spectroscopy. Fourier-transform infrared spectroscopy was applied to study the interaction of $rBPI_{21}$, and in some cases, PMB, with the hydrocarbon chains and phosphate groups of LPS, DMPG, and DMPC (DMPG and DMPC had to be chosen instead of PG and PC, because the latter two phospholipids do not exhibit an $\alpha \leftrightarrow \beta$ phase transition of the acyl chains in the physiological temperature range). In Figure 7, the peak position of $\nu_s(CH_2)$ is plotted versus temperature for F515 LPS suspensions in the presence of different concentrations of $rBPI_{21}$ (A) and PMB (B). Clearly, the phase transition temperature T_c at 32 °C for LPS of the *E. coli* Re mutant is shifted to higher temperatures in the presence of $rBPI_{21}$. This effect can already be observed at a molar ratio of [F515 LPS]:[$rBPI_{21}$] = 10:1 and increased with protein concentration. Concomitantly, a concentration-dependent decrease of the wavenumber values (corresponding to an increase of the state of order) over the whole temperature range occurred, indicating that the hydrophobic moiety of F515 LPS was rigidified. The effects of PMB on the acyl chains of F515 LPS were completely different: (i)

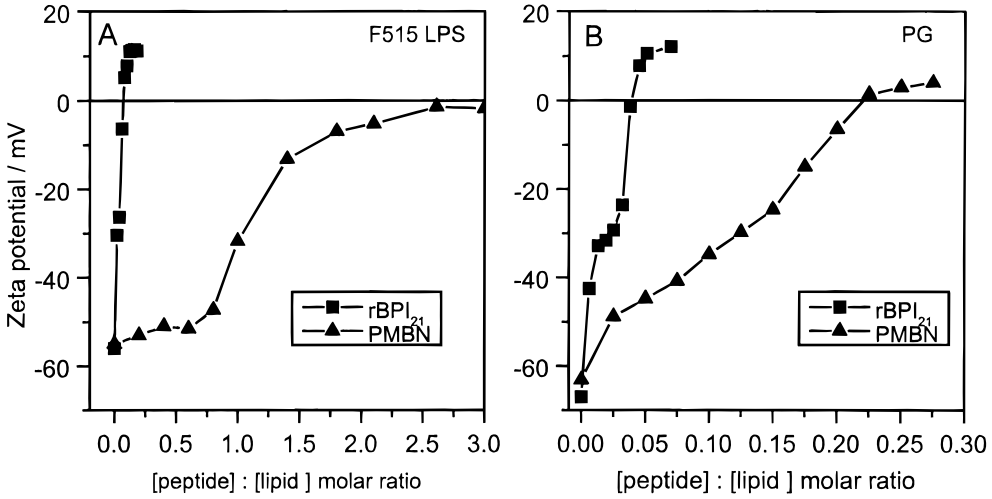

FIGURE 5: ζ-potential of 25 μM suspensions of F515 LPS (A) and PG (B) aggregates in dependence on the amount of $rBPI_{21}$ and PMBN, respectively, added to the aggregate suspensions. Buffer: 2.5 mM Tris/HCl and 1 mM CsCl, pH 7, T = 20 °C.

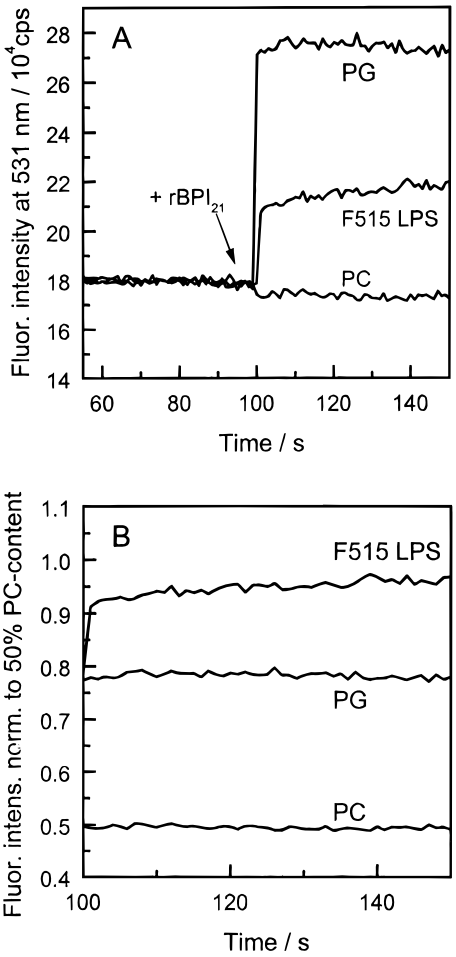

FIGURE 6: Change of the donor (NBD-PE) fluorescence intensities after addition of 2.4 μM $rBPI_{21}$ to 0.1 mM suspensions of PC, PG, or F515 LPS aggregates double-labeled with NBD-PE and Rh-PE in dependence on time. Buffer: PBS at pH 7.2, T = 37 °C.

no change of T_c could be observed except for the highest PMB concentration used, at which the phase transition disappeared, since the wavenumber values in the gel phase were raised to those typical for the liquid crystalline phase, (ii) in the gel phase, a concentration-dependent fluidization (increase in wavenumber values) occurred; and (iii) the molar F515 LPS-to-peptide stoichiometries required to induce a shift (e.g., by 2 wavenumbers) were 1:0.3 and 1:1, respectively. For R45 LPS and $rBPI_{21}$ similar effects could be observed (data not shown).

To obtain information on the lipid specificity of the $rBPI_{21}$ action, experiments with negatively charged (DMPG) and neutral zwitterionic phospholipids (DMPC) were also performed (Figure 8). For DMPG (Figure 8A), the action of $rBPI_{21}$ was similar to that observed for LPS (Figure 7A): T_c was increased and the acyl chains were rigidified in a concentration-dependent manner. For DMPC, however, T_c was left unchanged and the acyl chains were fluidized in both phases (Figure 8B). In contrast, the interaction of PMB with the two phospholipids led to a fluidization in the gel phase of DMPG but T_c was not affected, whereas in the case of DMPC no effects were observed (data not shown).

Since $rBPI_{21}$ and PMB are polycationic molecules, their interaction with the negatively charged phosphate groups of the lipids are likely to occur. To analyze this interaction, we studied the influence of the two compounds on the antisymmetric stretching vibration of the phosphate groups $\nu_{as}(PO_2^-)$ at 1260 cm^{-1}, which primarily corresponds to the undisturbed, weakly hydrated vibration. As shown in Figure 9, both compounds led to a reduction in the absorbance of the phosphate vibration of F515 LPS; however, to obtain a comparable reduction to that of $rBPI_{21}$ about 10-fold higher concentrations of PMB were required. This decrease of the band intensities can be interpreted to result from an immobilization of the phosphate groups due to binding of $rBPI_{21}$ or PMB, respectively. Also in this system, the action of $rBPI_{21}$ on DMPG was comparable to that on F515 LPS, whereas only a very small effect on DMPC was observed (data not shown).

DISCUSSION

BPI and its bioactive N-terminal fragments are bactericidal against a variety of Gram-negative bacteria (Ooi et al., 1987, 1991; Capodici et al., 1994; Gazzano-Santoro et al., 1992; Horwitz et al., 1996). From previous studies, BPI is known to bind to the outer membrane of these bacteria and to change their permeability toward molecules such as actinomycin D (Weiss et al., 1978). The action of BPI comprises several distinguishable phases. Whereas the binding of BPI triggers immediate alterations of the bacterial outer envelope, enhances the permeability toward actinomycin D, and inhibits

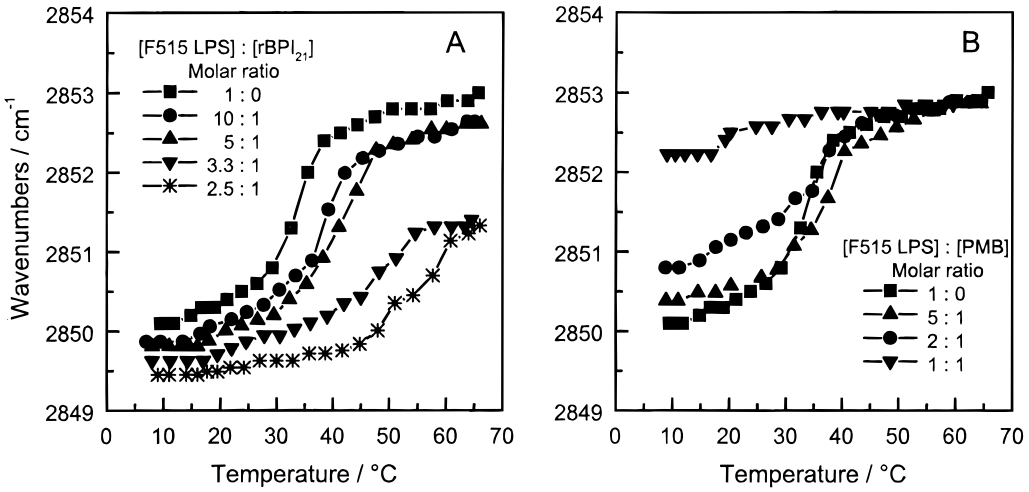

FIGURE 7: Peak position of the symmetric stretching vibration $\nu_s(CH_2)$ versus temperature for 10 mM F515 LPS suspensions in HEPES (5 mM) buffer in the presence of different amounts of $rBPI_{21}$ (A) and PMB (B).

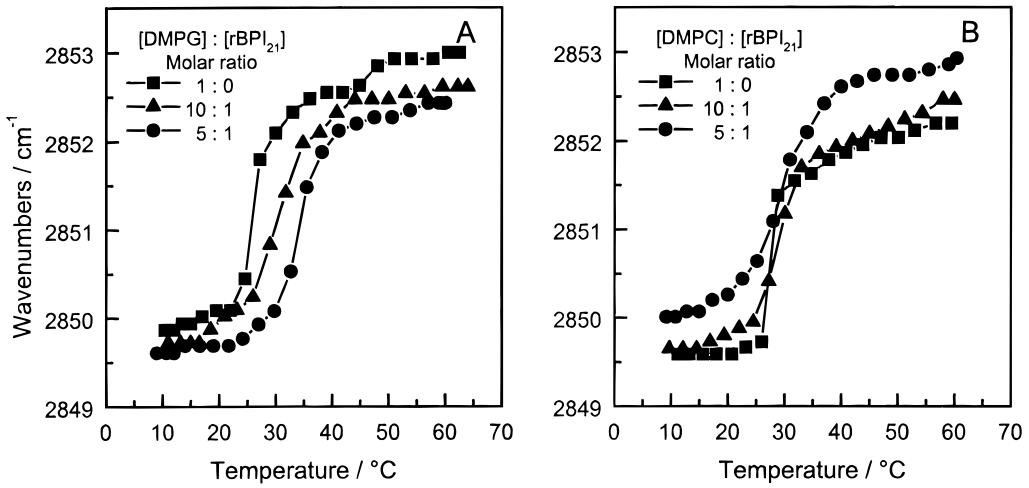

FIGURE 8: Peak position of the symmetric stretching vibration $\nu_s(CH_2)$ versus temperature for 10 mM DMPG (A) or DMPC suspensions in HEPES (5 mM) buffer (B) at different amounts of $rBPI_{21}$.

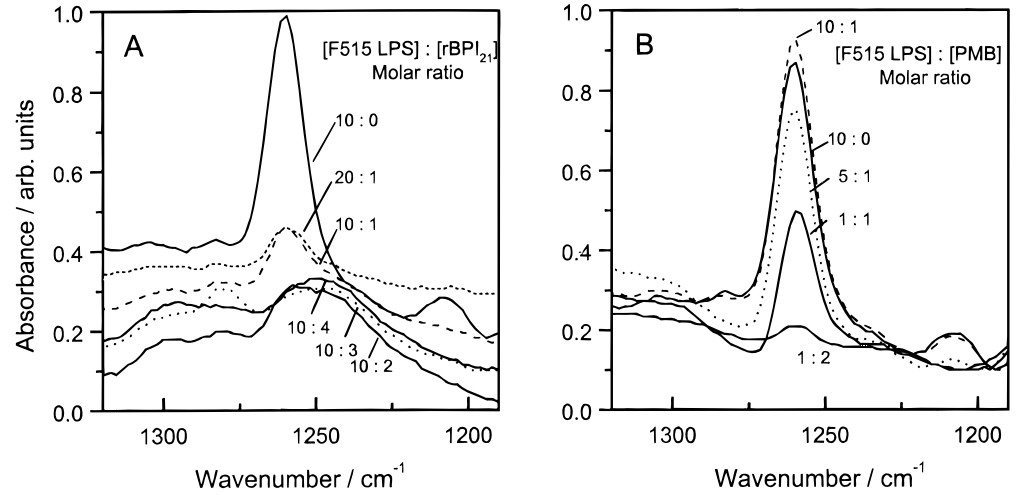

FIGURE 9: Infrared absorbance spectra for F515 LPS suspensions (10 mM) in HEPES (5 mM) buffer in the range of the antisymmetric stretching vibration of the negatively charged phosphates $\nu_{as}(PO_2^-)$ at 37 °C at different concentrations of $rBPI_{21}$ (A) or PMB (B).

the growth of susceptible microbes, the organisms exhibit little or no macromolecular degradation and remain capable of macromolecular biosynthesis for incubation periods of up to several hours. The sublethal effects of this initial phase can be reversed by addition of high concentrations of $MgCl_2$ ($\geq$40 mM) or 0.1% bovine serum albumin to the growth medium (Weiss et al., 1978; Mannion et al., 1990). This reversible phase is apparently followed by an irreversible one, which may be due to alterations of the cytoplasmic membrane (In't Veld et al., 1988). For these BPI effects, the molecular mechanisms remain to be determined. Recently, the N-terminal fragment $rBPI_{21}$ has attracted much attention as a possible therapeutic compound in Gram-negative infections (Huang et al., 1995; Horwitz et al., 1996;

Ammons & Mallari, 1996; Meijer et al., 1997; Kirsch et al., 1997).

On the basis of the present studies, we have determined characteristics of $rBPI_{21}$ that may play an important role in the interaction of $rBPI_{21}$ with bacterial membranes and thus may provide an explanation of the bactericidal effects of the protein.

The initial step in the interaction of $rBPI_{21}$ with membranes is its binding to the membrane surface. This step requires negative charges on the membrane surface as provided by negatively charged lipids. Weiss et al. (1983) have already discussed the role of charges in the action of BPI on Gram-negative bacteria, and de Kruiff (1994) has stressed the general important role of anionic phospholipids for the translocation of proteins into and across biological membranes. BPI binding should lead to a reduction in negativity of the surface potential, and as shown here, the negative ζ-potentials of PG and of F515 LPS aggregates are indeed even overcompensated upon addition of $rBPI_{21}$ (Figure 5). The protein concentration necessary to obtain saturation was roughly 2-fold lower for PG than for F515 LPS. Therefore, the saturating concentrations of the protein correlate with the surface charge densities of the two lipids [F515 LPS carries four net negative charges whereas PG carries only one, but the molecular area of F515 LPS (1.23 nm^2) is larger by a factor greater than 2]. Since functional properties of membrane proteins [e.g., porins (Wiese et al., 1994; Brunen & Engelhardt, 1995)] are influenced by the transmembrane potential and surface charges (Gallin & McKinney, 1990), these data not only confirm the binding of $rBPI_{21}$ but also may contribute to an understanding of the bactericidal activity of the protein.

In all lipids used in the present investigations, the negative charges were represented by phosphate residues, and in F515 and R45 LPS additionally by carboxyl groups. Binding of $rBPI_{21}$ led to the immobilization of the phosphate groups (Figure 9), showing their importance in the interaction of $rBPI_{21}$ with the lipids. In accordance with this interpretation are the effects of $rBPI_{21}$ on the neutral phospholipid DMPC. Future experiments will examine whether $rBPI_{21}$ induces similar effects with lipids in which the negative charge is represented by other negatively charged functional groups.

The second step in the interaction of $rBPI_{21}$ with the membrane is its intercalation into the membrane from the aqueous phase. This leads in monolayer experiments to an increase in film area of the negatively charged lipids LPS and DMPG (Figure 3). The significantly larger increase in film area seen with F515 LPS monolayers is due to the higher surface charge density. This holds also for R45 LPS, even though the effect is less pronounced. Obviously, $rBPI_{21}$ incorporation into the various monolayers is correlated with their surface charge density. The significance of negative surface charges or surface charge densities is further supported by the protective effect of $MgCl_2$ on the incorporation of $rBPI_{21}$ into F515 LPS monolayers (Figure 4). Interestingly, the concentration of $rBPI_{21}$ in the subphase required for the induction of significant effects (2.5 nM, corresponding to 53 ng/mL) was more than 2 orders of magnitude lower than BPI concentrations observed in body fluids of abscess cavities harboring Gram-negative and Gram-positive bacterial species (up to some micrograms per milliliter) (Opal et al., 1994) or $rBPI_{23}$ peak levels after infusion with $rBPI_{23}$ (up to 10 μg/ml) (Bauer et al., 1996) but significantly higher than BPI plasma levels of healthy humans (typically less than 1 ng/mL) (Froon et al., 1995; White et al., 1994). However, due to electrostatic attraction involved in the interaction between $rBPI_{21}$ and negatively charged lipids, an accumulation of the BPI_{21} molecules at the surface of the lipid layer might occur. The comparatively high amounts of $rBPI_{21}$ used in the RET, ζ-potential, and in particular the FTIR experiments (up to 168 mg/mL) were needed because of the high lipid concentration in the sample suspensions (up to 50 mg/mL).

The slight increase in film area at lateral pressures below 25 mN/m of monolayers made from DMPC is likely due to the surface activity of the protein itself, i.e., $rBPI_{21}$ itself forms protein monolayers at the air/water interface (Figure 2). The course of the isotherms indicates that at lateral pressures above approximately 35 mN/m the protein is excluded from the monolayer into the subphase. This is in accordance with measurements of the surface tension of $rBPI_{21}$ suspensions and the dependence on protein concentration. Here, a maximal reduction of surface tension from 72 mN/m (protein-free subphase) to about 40 mN/m could be achieved (unpublished results). Thus, the difference in surface tension of 32 mN/m agrees well with the maximal lateral pressure of 35 mN/m.

The intercalation of $rBPI_{21}$ into lipid matrices is further supported by the RET measurements, which showed that the protein intercalated into the negatively charged F515 LPS and PG aggregates but not into neutral PC aggregates (Figure 6). In accord with the surface charge density of the lipids, the amount of incorporated $rBPI_{21}$ is maximal for the F515 LPS aggregates. However, a quantitative calculation of the amount of protein molecules inserted into the F515 LPS matrix cannot be performed, since this requires a calibration of the changes in fluorescence intensity in relation to protein concentration. For this, a preparation of mixed aggregates from a given amount of F515 LPS together with a known amount of $rBPI_{21}$ molecules in the chloroform phase would be required. It is likely, however, that the protein would not tolerate this procedure unaltered.

As found in the present studies, a dramatic effect of $rBPI_{21}$ on membrane systems is the rigidification of acyl groups. The different effects on the acyl chain mobility upon the intercalation of $rBPI_{21}$ and of PMB into the hydrophobic moiety of the target lipid assemblies may depend on the hydrophobicity, the net positive charge, and the size of the two peptides. $rBPI_{21}$ appears to intercalate deeply into the hydrocarbon moiety and causes its rigidification, as indicated by the shift in the wavenumbers of the $\nu_s(CH_2)$ vibration to lower values and a shift of T_c to higher temperatures with increasing protein concentration (Figure 7A). Interestingly, the magnitude of these effects at comparable $rBPI_{21}$ concentrations were similar for both types of LPS and DMPG. This surprising observation finds its explanation when the particular sample preparation for the FTIR measurements is considered: lipid and protein are vortexed together in a small volume at relatively high molar concentrations, whereas in all other experiments the protein was added to a larger volume of equilibrated lipid systems. In the latter systems, the local concentrations of the protein reached in the lipid matrix are again strongly dependent on the negative surface charge density.

In contrast to $rBPI_{21}$, similar experiments with PMB show a concentration-dependent fluidization of the acyl chains of

F515 LPS and DMPG and no influence on T_c (Figure 7B). These observations can be explained by assuming that the PMB molecules, the positive charges of which are exclusively located on the amino acids, bind to the interface region of the lipids, thus acting as spacer molecules and providing more space for the hydrocarbon chains of the lipids and, subsequently, allowing a higher mobility (fluidity). This comparison leads to the conclusion that, due to the intercalation of $rBPI_{21}$, the space within the hydrophobic moiety of the lipids is reduced.

Following the interaction with DMPC, $rBPI_{21}$ increases the fluidity of the acyl chains in both phases in a concentration-dependent manner, whereas T_c remains unchanged. Though DMPC carries a phosphate group, the negative charge is neutralized by the choline. The increase of the fluidity of DMPC acyl chains, in contrast to a decrease in the case of LPS and DMPG, might be due to the smaller electrostatic interaction with DMPC, which leads to a less deep intercalation of the protein into the hydrophobic moiety. Thus, $rBPI_{21}$ proteins may not interact directly with the acyl chains but rather lead to a separation of the lipid headgroups allowing a higher mobility of the hydrocarbon chains.

The results discussed so far for the lipid specificity clearly show that $rBPI_{21}$ interacts not only with F515 LPS but also with R45 LPS. This agrees with the reported binding capacities of the protein and its antibacterial activities, which were shown to be comparable for *E. coli* strain J5 and *P. mirabilis* strain R45 (Capodici et al., 1994). Furthermore, from our results it may be concluded that the action of $rBPI_{21}$ is not restricted to LPS but rather extends to negatively charged lipids in general. This is true despite the observations that the binding affinity of BPI to immobilized LPS (Gazzano-Santoro et al., 1992, 1995) and to the outer membrane of intact bacteria (Capodici et al., 1994; Gazzano-Santoro et al., 1994) is high. In view of the fact that the protein, besides being hydrophobic, expresses properties of a polycationic molecule, this is not surprising. Importantly, however, infusion of the related protein $rBPI_{23}$ in human endotoxin challange studies was well tolerated (von der Möhlen et al., 1995).

Our findings could also explain the effects of BPI on isolated bacterial cytoplasmic membrane vesicles as described by In't Veld et al. (1988). In this study it was shown that BPI disrupted the functional integrity (inhibition of lactate-dependent proline uptake, efflux of previously accumulated proline, and changes in O_2 consumption in the presence of lactate) of the cytoplasmic membranes of both Gram-negative and BPI-insensitive Gram-positive bacteria. Similarly, Horwitz and Nadell (1995) have shown that, in addition to intact Gram-negative bacteria, BPI is cytotoxic to mycoplasma and L-forms of Gram-positive bacteria. The detection of surface-associated BPI on mononuclear cells by Dentener et al. (1996) would also be in accordance with an affinity of BPI for negatively charged phospholipids. Furthermore, the intercalation of $rBPI_{21}$ into phospholipid liposomes resembling the lipid composition of macrophages fits this picture (Schromm et al., 1996). It should be emphasized, however, that in all experiments involving $rBPI_{21}$ interacting with membrane surfaces from the aqueous environment, $rBPI_{21}$ exhibited a significantly higher activity toward LPS because of its higher negative surface charge density.

From the evaluation of pressure/area isotherms of monolayers formed from pure $rBPI_{21}$ suspensions, the molecular area of one protein molecule was estimated as 11.8 ± 3.9 nm^2 at a lateral pressure of 25 mN/m (Figure 2). At this lateral pressure the addition of 10 nM $rBPI_{21}$ (corresponding to 2.4×10^{14} molecules) into the subphase led to an increase in film area of the F515 LPS monolayer from 22.1 cm^2 to 31.2 cm^2 (Figure 3A). As the data of Figure 2B suggest, this increase in area corresponds to the incorporation of 8.4×10^{13} $rBPI_{21}$ molecules. This calculation shows that, under the applied experimental conditions, 35% of the protein molecules were incorporated into the monomolecular film and that the stoichiometry of $rBPI_{21}$ and F515 LPS in the film is approximately 1:21. In the case of R45 LPS the increase in monolayer area induced by the same amount of protein was only half that observed for F515 LPS, yielding a stoichiometry of approximately 1:42. This corresponds approximately to the lower surface charge density of R45 LPS as compared to F515 LPS. This implies that only part of the LPS molecules are actually complexed by $rBPI_{21}$ and that the interaction leads to a lateral separation of domains of complexed and noncomplexed LPS. A respective estimation for DMPG leads to an even higher ratio in favor of the lipid.

It must, however, be taken into consideration that these data are only rough estimates for an $rBPI_{21}$:LPS stoichiometry because the incorporation of $rBPI_{21}$ into the monolayer could lead to a structural rearrangement of the protein resulting in a molecular area differing from that deduced from the pure $rBPI_{21}$ monolayers. Furthermore, within the 30 min waiting period until the compression isotherms were continued, not all of the protein may have interacted with the monolayer. These facts may explain the differences between the stoichiometric data from monolayer measurements and the higher ratios (factor of 2) obtained from the saturation values of the ζ-potential (Figure 5). Although the latter method would require the knowledge of the $rBPI_{21}$ distribution within the different lipid layers in the aggregates (is it restricted to the surface or does it move into inner lipid layers?), we could conclude that the $rBPI_{21}$:LPS ratios are well below 1:2 and are, thus, in contrast to those determined with intact bacteria (Gazzano-Santoro et al., 1994) from the ratio of the amount of bound BPI and the number of LPS molecules per bacterium.

The stabilizing effect of $MgCl_2$ is interesting also in another aspect. It has been reported that $10-20$ mM $MgCl_2$ protect against the permeability-increasing effects of BPI obtained either from rabbit (Weiss et al., 1975, 1983, 1984) or human granulocytes (Weiss et al., 1978) toward the antibiotic actinomycin D. Surprisingly, $MgCl_2$ did not influence the binding of BPI to isolated LPS, whereas its binding to the surface of intact bacteria was inhibited (Weiss et al., 1975). We show here that high concentrations of $MgCl_2$ (40 mM) in the bathing solution of the membranes lead to their protection against the action of $rBPI_{21}$ (Figure 4), providing supportive evidence for the protective role of Mg^{2+} ions.

In summary, our data show that $rBPI_{21}$ binds to negatively charged lipids and most strongly to F515 LPS. The binding is followed by the deep intercalation of the protein into the hydrophobic interior of the membrane, causing immobilization of the hydrocarbon chains. Furthermore, the intercalation leads to large changes in the surface potential, which

may influence the gating behavior of outer membrane proteins. These effects may also occur in the bacterial membrane and participate in their dysfunction.

ACKNOWLEDGMENT

We are indebted to D. Koch and G. von Busse for performing the film balance and infrared spectroscopic measurements and to Mrs. M. Lohs for the preparation of the drawings.

REFERENCES

Ammons, W. S., & Mallari, C. (1996) *J. Endotoxin Res. 3*, 57−66.
Bauer, R. J., White, M. L., Wedel, N., Nelson, B. J., Friedmann, N., Cohen, A., Hustinx, W. N. M., & Kung, A. H. C. (1996) *Shock 5*, 91−96.
Beurer, G., Warncke, F., & Galla, H.-J. (1988) *Chem. Phys. Lipids 47*, 155−163.
Blume, A. (1979) *Biochim. Biophys. Acta 557*, 32−44.
Brandtzaeg, P. (1996) in *Pathology of Septic Shock* (Rietschel, E. T., & Wagner, H. Eds.) pp 15−37, Springer-Verlag, Berlin, Heidelberg, and New York.
Brunen, M., & Engelhardt, H. (1995) *FEMS Microbiol. Lett. 126*, 127−132.
Capodici, C., Chen, S., Sidorczyk, Z., Elsbach, P., & Weiss, J. (1994) *Infect. Immun. 62*, 259−265.
Cevc, G. (1990) *Biochim. Biophys. Acta 1031*, 311−382.
Cevc, G. (1993) *Chem. Phys. Lipids 64*, 163−186.
de Kruijff, B. (1994) *FEBS Lett. 346*, 78−82.
de Winter, R. J., von der Möhlen, M., van Lieshout, H., Wedel, N., Nelson, B., Friedmann, N., Delemarre, B. J. M., & van Deventer, S. J. H. (1995) *J. Inflammation 45*, 193−206.
Dentener, M. A., Francot, G. J. M., & Buurman, W. A. (1996) *J. Infect. Dis. 173*, 232−235.
Elsbach, P., & Weiss, J. (1993) *Immunobiology 187*, 417−429.
Elsbach, P., Weiss, J., Franson, R. C., Beckerdite-Quagliata, S., Schneider, A., & Harris, L. (1979) *J. Biol. Chem. 254*, 11000−11009.
Froon, A. H. M., Dentener, M. A., Greve, J. W. M., Ramsay, G., & Buurman, W. A. (1995) *J. Infect. Dis. 171*, 1250−1257.
Galanos, C., Lüderitz, O., & Westphal, O. (1969) *Eur. J. Biochem. 9*, 245−249.
Gallin, E. K., & McKinney, L. C. (1990) in *Current Topics in Membranes and Transport* (Grinstein, S., & Rotstein, O. D., Eds.) pp 127−152, Academic Press, New York.
Gazzano-Santoro, H., Parent, J. B., Grinna, L., Horwitz, A., Parsons, T., Theofan, G., Elsbach, P., Weiss, J., & Conlon, P. J. (1992) *Infect. Immun. 60*, 4754−4761.
Gazzano-Santoro, H., Mészáros, K., Birr, C., Carroll, S. F., Theofan, G., Horwitz, A. H., Lim, E., Aberle, S., Kasler, H., & Parent, J. B. (1994) *Infect. Immun. 62*, 1185−1191.
Gazzano-Santoro, H., Parent, J. B., Conlon, P. J., Kasler, H., Tsai, C.-M., Lill-Elghanian, D. A., & Hollingsworth, R. I. (1995) *Infect. Immun. 63*, 2201−2205.
Hansbrough, J., Tenenhaus, M., Wikström, T., Braide, M., Rennekampff, O. H., Kiessig, V., & Bjursten, L. M. (1996) *J. Trauma 40*, 886−892.
Horwitz, A. H., & Nadell, R. (1995) in *Proceedings of the 95th Meeting of the American Society for Microbiology*, abstr. E-1, p 280, Washington, DC.
Horwitz, A. H., Leigh, S. D., Abrahamson, S., Gazzano-Santoro, H., Liu, P.-S., Williams, R. E., Carroll, S. F., & Theofan, G. (1996) *Protein Expression Purif. 8*, 28−40.
Huang, K., Fishwild, D. M., Wu, H.-M., & Dedrick, R. L. (1995) *Inflammation 19*, 389−404.
Hunter, R. J. (1981) in *Zeta potential in colloid science*, Academic Press, London.
In't Veld, G., Mannion, B., Weiss, J., & Elsbach, P. (1988) *Infect. Immun. 56*, 1203−1208.
Kartalija, M., Kim, Y., White, M. L., Nau, R., Tureen, J. H., & Täuber, M. G. (1995) *J. Infect. Dis. 171*, 948−953.
Kirsch, E., Quint, P., Carroll, S., Scannon, P., Giroir, B., & BPI Study Group (1997) *Shock 7* (Suppl.), 142.
Koyama, S., Shibamoto, T., Ammons, W. S., & Saeki, Y. (1995) *Shock 4*, 74−78.
Lechner, A. J., Lamprech, K. E., Johanns, C. A., & Matuschak, G. M. (1995) *Shock 4*, 298−306.
Mannion, B. A., Weiss, J., & Elsbach, P. (1990) *J. Clin. Invest. 85*, 853−860.
Mantsch, H. H., & McElhaney, R. N. (1991) *Chem. Phys. Lipids 57*, 213−226.
Marcelja, S. (1974) *Biochim. Biophys. Acta 367*, 165−176.
Meijer, C., Hack, C. E., Wedel, N. I., Thijs, L. G., Wiezer, M. J., Wünsche, R., Wiggers, T., Zoetmulder, F. A. N., Borelrinkes, I. H. M., Gouma, D. J., Cuesta, M. A., Nelson, B. J., Havrilla, M., Meijer, S., & van Leeuwen, P. A. M. (1997) *Shock 7* (Suppl.), 159.
Ooi, C. E., Weiss, J., Elsbach, P., Frangione, B., & Mannion, B. (1987) *J. Biol. Chem. 262*, 14891−14894.
Ooi, C. E., Weiss, J., Doerfler, M. E., & Elsbach, P. (1991) *J. Exp. Med. 174*, 649−655.
Opal, S. M., Palardy, J. E., Marra, M. N., Fisher, C. J., Jr., McKelligon, B. M., & Scott, R. W. (1994) *Lancet 344*, 429−431.
Rietschel, E. T., Kirikae, T., Schade, F. U., Mamat, U., Schmidt, G., Loppnow, H., Ulmer, A. J., Zähringer, U., Seydel, U., Di Padova, F., Schreier, M., & Brade, H. (1994) *FASEB J. 8*, 217−225.
Schromm, A. B., Brandenburg, K., Rietschel, E. T., Flad, H.-D., Carroll, S. F., & Seydel, U. (1996) *FEBS Lett. 399*, 267−271.
Schröder, G., Brandenburg, K., & Seydel, U. (1992) *Biochemistry 31*, 631−638.
Schwarz, G., & Taylor, S. E. (1995) *Langmuir 11*, 4341−4346.
Struck, D. K., Hoekstra, D., & Pagano, R. E. (1981) *Biochemistry 20*, 4093−4099.
Vinogradov, E. V., Thomas-Oates, J. E., Brade, H., & Holst, O. (1994) *J. Endotoxin Res. 1*, 199−206.
von der Möhlen, M. A. M., Kimmings, A. N., Wedel, N. I., Mevissen, M. L. C. M., Jansen, J., Friedmann, N., Lorenz, T. J., Nelson, B. J., White, M. L., Bauer, R., Hack, C. E., Eerenberg, A. J. M., & van Deventer, S. J. H. (1995) *J. Infect. Dis. 172*, 144−151.
Weiss, J., & Olsson, I. (1987) *Blood 69*, 652−659.
Weiss, J., Franson, R. C., Beckerdite, S., Schmeidler, K., & Elsbach, P. (1975) *J. Clin. Invest. 55*, 33−42.
Weiss, J., Elsbach, P., Olsson, I., & Odeberg, H. (1978) *J. Biol. Chem. 253*, 2664−2672.
Weiss, J., Victor, M., & Elsbach, P. (1983) *J. Clin. Invest. 71*, 540−549.
Weiss, J., Muello, K., Victor, M., & Elsbach, P. (1984) *J. Immunol. 132*, 3109−3115.
Weiss, J., Elsbach, P., Shu, C., Castillo, J., Grinna, L., Horwitz, A., & Theofan, G. (1992) *J. Clin. Invest. 90*, 1122−1130.
White, M. L., Ma, J. K., Birr, C. A., Trown, P. W., & Carroll, S. F. (1994) *J. Immunol. Methods 167*, 227−235.
Wiese, A., Schröder, G., Brandenburg, K., Hirsch, A., Welte, W., & Seydel, U. (1994) *Biochim. Biophys. Acta 1190*, 231−242.
Wiese, A., Brandenburg, K., Carroll, S. F., Rietschel, E. T., & Seydel, U. (1997) *Biochemistry 36*, 10311−10319.
Zähringer, U., Lindner, B., Seydel, U., Rietschel, E. T., Naoki, H., Unger, F. M., Imoto, M., Kusumoto, S., & Shiba, T. (1985) *Tetrahedron Lett. 26*, 6321−6324.

BI970176M